24th COBEM - 2017

24th ABCM International Congress of Mechanical Engineering
December 3-8, 2017, Curitiba, PR, Brazil

COBEM-2017-2640
DYNAMIC CONSIDERATIONS FOR ENGINE'S CHARTS AND APPLICATION AT EMB-314 AND NORTHROP F-5F AIRCRAFT

Guilherme Soares e Silva
Diego Serra Azul de Albuquerque
Flávio José Silvestre
Instituto Tecnológico de Aeronáutica - ITA
soaresgss@it.br, diegoserraazul@gmail.com, flaviojs@ita.br

Alan Fonseca Uehara
Instituto de Pesquisa e Ensaios em Voo - IPEV
alanafu@ipev.cta.br

Abstract. *The knowledge of how the propulsive force dynamically behaves is helpful to improve models with accuracy. It is particularly important for high performance aircraft and for flight test activity. For high performance aircraft that have a high power-to-weight ratio, the thrust effects on the aircraft dynamics are of major importance, and must be deeply investigate. Due to risks associate to flight testing, models with improve accuracy must be used to detect unsafe flight conditions a priori. This study deals with these two issues above. Through a dynamic thrust model proposed based on engine's performance charts, it is intended to validate the expansion of the operational envelope from engine of EMB-314 and verify the model accuracy for transient thrust response for Northrop F-5F. In both cases data from real flight tests are used.*

Keywords: *Dynamic thrust, Thrust, Propulsion System, A-29, Super Tucano, EMB 314, Hartzell, PT6A-68C, Flight Test, Northrop F-5F, GE J85-21, engine's charts*

1. INTRODUCTION

This work aims to develop a thrust model using dynamical considerations for small variations around a thrust regime. The model proposed is based on engines performance charts. This model shall improve the aircraft simulation providing a reliable tool for flight test analyses.

Generally, a flight simulator uses manufactures engine charts, the engine deck, as a thrust model. In the specific of propulsive systems whose architecture has the propeller as a thrust generator, the thrust is calculated considering dimensionless coefficients determined in static tests.

The proposed model in this paper intends to change this deck to improve fidelity of the aircraft dynamical response. The use of the model will be demonstrated for two different aircraft models in different applications. The first one is for the expansion of the flight envelope of the high-performance trainer EMB-314 Super Tucano.The second application compares simulations results using the proposed model for the aircraft Northrop F-5F with flight test data.

2. THEORETICAL FORMULATION

2.1 Point-mass equations of motion

The equations of motion for an aircraft in steady flight according to the point-mass approximation, considering the aerodynamic reference frame, are given by equations (1) and (2) (Vinh, 1999).

$$L + Tsen(\alpha) = n_{za}W \tag{1}$$

$$Tcos(\alpha) - D = -n_{xa}W \tag{2}$$

Where,α is the angle of attack, D stays for drag force, L for the lift, n_{xa} and n_{za} are the load factors in x- and z-axes, T is the thrust and W is the weight.

With a known polar drag for a specific flight condition (flight velocity, altitude, weight and load factors), equations (1) and (2) may be used to obtained the thrust as a function of the aircraft state. Explicitly the necessary thrust of to flight in

a trimmed condition can be obtained solving equations. (3), (4) and (5), where C_L is the lift coefficient, C_D is the drag coefficient as a function of C_L, P_a stays for atmospheric pressure, S is the wing area, M is the mach number and γ is the poisson constant.

$$C_L = \frac{n_{za}W - Tsen(\alpha)}{(\gamma/2)SP_aM^2} \tag{3}$$

$$D = \frac{\gamma}{2}SP_aM^2C_D(C_L) \tag{4}$$

$$T = \frac{D - n_{xa}W}{cos(\alpha)} \tag{5}$$

2.2 Linearization around equilibrium point

For the same throttle position, Eq. (5) may be expanded around an equilibrium point using a first order Taylor series, as shown in Eq. (6). The equilibrium point is referred to by the index **o**.

$$T = \left(\frac{D_o - n_{xa_o}Wo}{cos(\alpha_o)}\right) + \frac{\partial T}{\partial n_{x_a}}\Big|_o(n_{x_a} - n_{x_{a_o}}) + \frac{\partial T}{\partial D}\Big|_o(D - D_o) + \frac{\partial T}{\partial \alpha}\Big|_o(\alpha - \alpha_o) + \frac{\partial T}{\partial W}\Big|_o(W - W_o) \tag{6}$$

Combining equations (6) and (5), the thrust can be obtained as following.

$$T = T_o + \frac{D - D_o - W_o(n_{x_a} - n_{x_{a_o}}) - n_{x_{a_o}}(W - W_o) + tan(\alpha_o)(D_o - n_{x_{a_o}}W_o)(\alpha - \alpha_o)}{cos(\alpha_o)} \tag{7}$$

In Eq. (7), T_o represents the thrust value in the equilibrium condition.

2.3 The engines chart

It's possible to determine the thrust generated by an engine from engine parameters and flight conditions. The listed values for the thrust are obtained experimentally through static tests accomplished under controlled conditions. The aircraft manufacturer has access to these data for engine's integration and in the aircraft development process.

For propellers, thrust is a function of propeller diameter, angular velocity (RPM), flow conditions and shaft power generated in the engine as in Eq. (8). Generally, thrust is given by non-dimensional coefficients as shown in Eq. (9). This thrust coefficient in turn is a of non-dimensional parameters as the Mach number at propeller tip, the power coefficient and the advance ratio.

$$T = f(P_a, D_p, \omega, \rho, V_{TAS}, T_a) \tag{8}$$

$$C_T = \frac{T}{\rho\omega^2 D_p^4 f_B} \tag{9}$$

Where, C_T is the thrust coefficient, D_p is the propeller diameter, f_B is the body correction factor, ρ is the air density, T_a is ambient temperature, V_{TAS} stays for true air speed and ω is the propeller angular velocity.

Combining equations (9) and (7), we can obtain Eq. (10).

$$C_T = C_{T_o} + \frac{1}{\rho\omega^2 D_p^4 f_B cos(\alpha_o)}\left[(n_{x_a} - n_{x_{a_o}})W_o + tan(\alpha_o)(\alpha - \alpha_o)(D_o + n_{x_{a_o}}W_o) + D - D_o\right] \tag{10}$$

Analyzing Eq. (10), it is possible to conclude that the first part representing static conditions is equivalent to information provided by the engine's chart, i.e. the trimming thrust. In addition, this equation shows the importance of dynamic considerations in order to carry out simulations that require variations of flight condition. Thus, monitoring online the load factor n_{xa} and the angle of attack α, and using the aircraft drag polar, dynamic thrust can be calculated.

3. MODEL APPLICATION

3.1 Expansion of Pratt & Whitney PT6A-68C manufacturer's engine deck with the aircraft EMB-314

The proposed model is applied in the extrapolation of Pratt & Whitney PT6A-68C manufacturer's engine deck and this envelope extrapolation is validated with flight test data of EMB-314 Super Tucano. This is a turboprop engine with maximum shaft power of 1600SHP and is equipped with a 5-blade Hartzell propeller that is integrated in the EMB-314.

In view of the fact that the engines chart does not entirely cover the operational envelope, the analysis of its extrapolation and further application in flight simulators is recommended. Rewriting Eq. (10), the trimmed thrust coefficient can be determined as follows:

$$C_{T_o} = C_T - \frac{1}{\rho\omega^2 D_p^4 f_B cos(\alpha_o)} \left[(n_{x_a} - n_{x_{a_o}})W_o + tan(\alpha_o)(\alpha - \alpha_o)(D_o + n_{x_{a_o}}W_o) + D - D_o\right] \tag{11}$$

Now, C_T can be obtained from equations (3) to (5), and subtraction between this coefficient and the dynamic part of the thrust coefficient accordiung the proposed model, the trimmed coefficient C_{To} can be recovered and compared to the engine chart values.

3.1.1 Flight test campaign

A flight test campaign has be accomplished with the aircraft EMB-314 Super Tucano focused in low-torque conditions, not covered from the engine chart. The aircraft flew with land gear up and flaps retracted, with environment control system turned on. During the flight test tasks, the intention was to performed a descending flight-path with constant velocity and constant engine set.

In Tab. 1, the configurations for the planned tasks are shown in detail.

Table 1. Flight conditions and results for flight test tasks

Task#	T_q[%]	CAS[1] [m/s]	Zp [m]	$max\frac{\lvert T_d - T_c\rvert}{T_d}$ [2][%]	$max\frac{\lvert T_d - T_{mod}\rvert}{T_d}$ [3] [%]
1	4	86	6.500	461,7	4,8
2	6	78	3.800	713,8	5,7

(1) Calibrated Air Speed
(2) Maximum error between thrust from engine chart and kinematic calculation relative to engine chart
(3) Maximum error between thrust from engine chart and proposed model relative to engine chart

3.1.2 Results and analyses

The results obtained in this flight test campaign are summarized in the following. In Fig.1 the calibrated airspeed of task 1 can be seeing oscillating around 86.5 m/s, while the altitude is decreasing. In Fig.2 the thrust according to the proposed model is shown and used to calculate the static thrust for several points in time. This static thrust curve is compared to the constant thrust according engines deck expansion the good agreement reveals that the proposed model was able to represent the dynamic effects for the entire maneuver. Correspondingly, similar results are shown in Fig.3 for the thrust coefficient. For the second task, the results are shown in Fig.4 to 6. It can be observed that for a different flight condition, the proposed model is still able to represent the thrust dynamic effects.

Overall, the dynamic thrust can oscillate up to 460% of static one. The maximum differences between the static thrust calculated from the proposed model and through expansion of the engine chart was 5,7%.

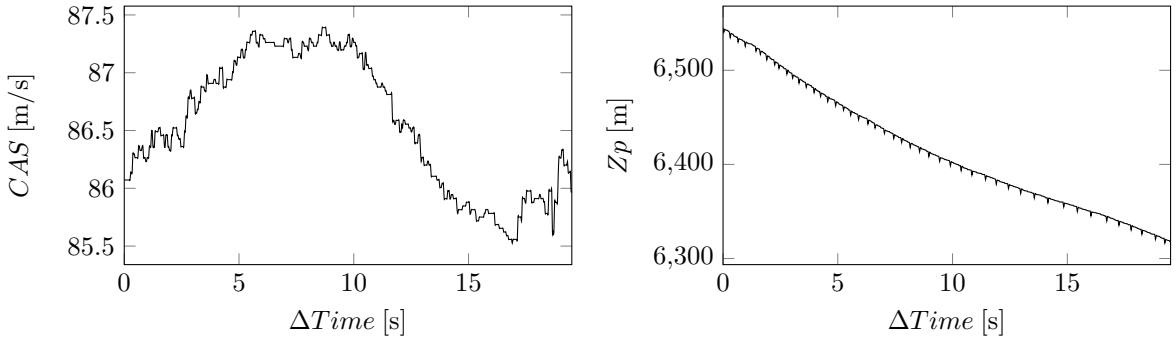

Figure 1. Evolution of Calibrate Air Speed (CAS) and Altitude (Z_p) on task number 1

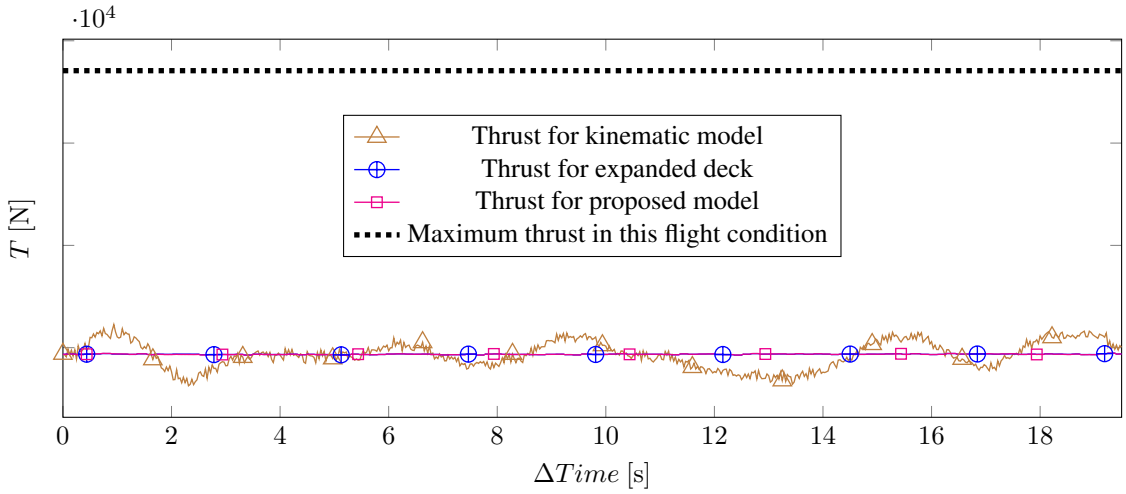

Figure 2. Thrust for kinematics conditions, for proposed model and for extrapolled deck on task 1 flight conditions

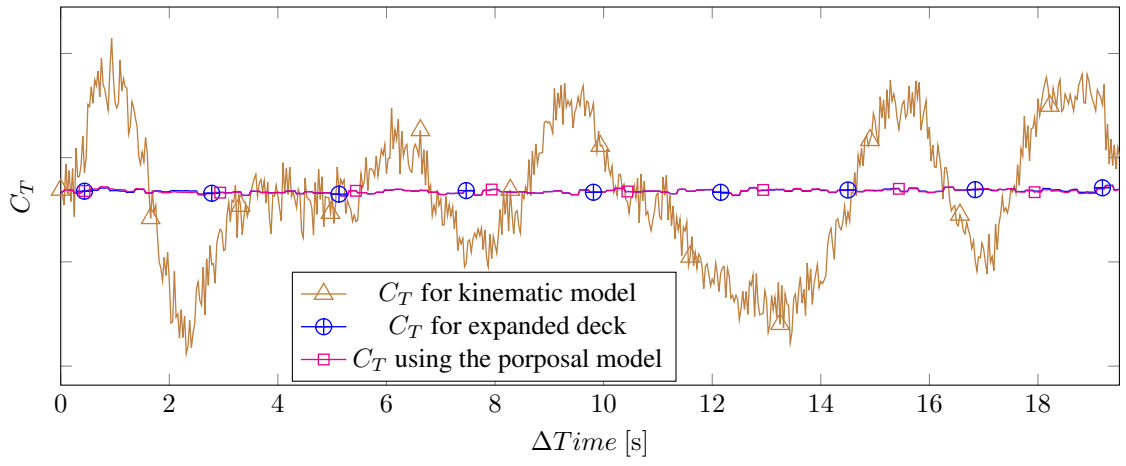

Figure 3. Thrust coefficient for kinematics conditions, for proposed model and for extrapolate deck on task 1 flight conditions

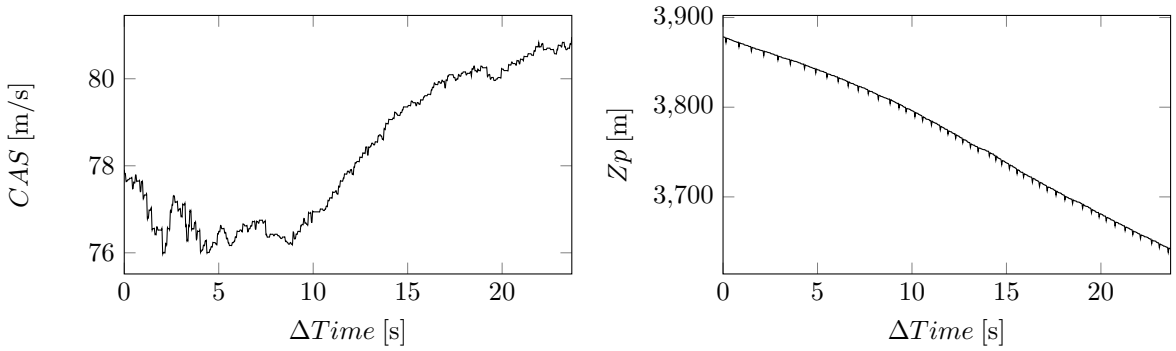

Figure 4. Evolution of Calibrate Air Apeed (CAS) and Altitude (Z_p) on task number 2

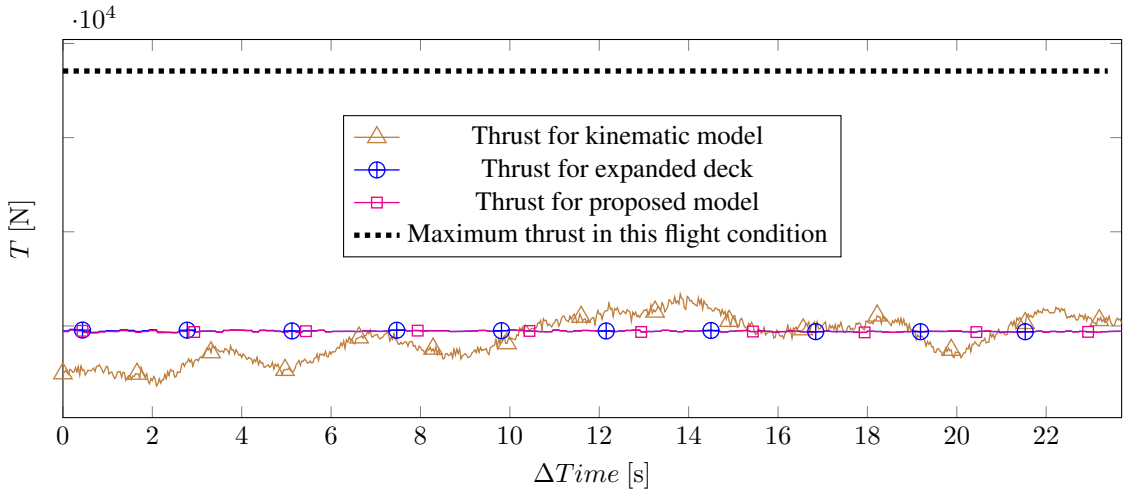

Figure 5. Thrust for kinematics conditions, for proposed model and for extrapolate deck on task 2 flight conditions

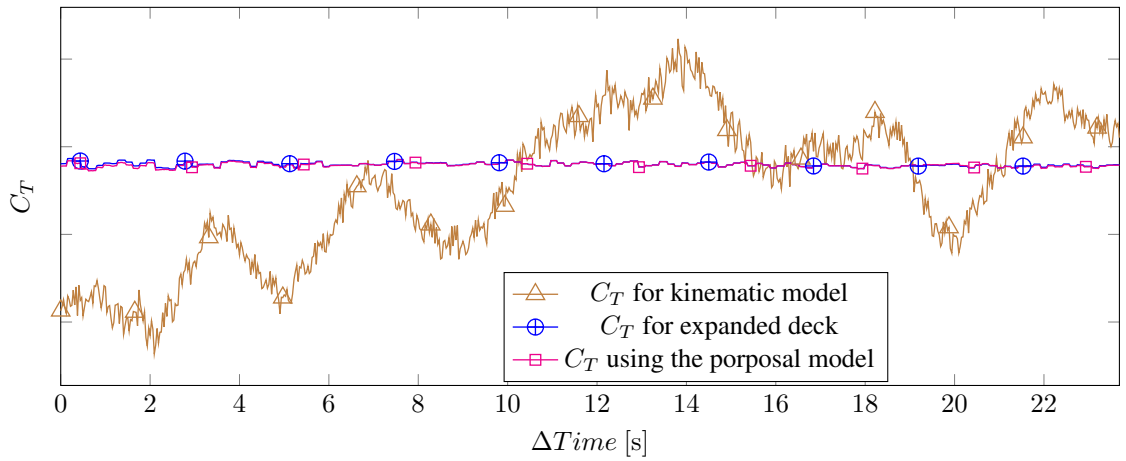

Figure 6. Thrust coefficient for kinematics conditions, for proposed model and for extrapolate deck on task 2 flight conditions

3.2 Transient thrust of GE J85-21 engine with the aircraft Northrop F-5F

The GE J85-21 is a turbojet engine with 1474 kg maximum thrust in military condition - when in afterburner set the engine can reach up to 2109 kg. The engine is equipped with a control system for variable geometry exhaust nozzle and auxiliary air inlets. Two of this engines are integrated in the Northrop F-5F.

In this analysis the objective is to compare the proposed model and the engine chart responses in a transient condition, i.e. when thrust is varying. The kinematic calculation of the thrust is used as a reference value. The drag polar used for this study is given by Silva *et al.* (2015). As the value for the thrust in the equilibrium condition, the increased thrust after

the step command was used.

3.2.1 Flight test campaign

The aircraft flew with landing gear and flaps retracted, and 275 gallon external fuel tank on aircraft centerline (under the fuselage). During each task, the aircraft changed the thrust condition from power for the level flight to the maximum thrust without afterburner (military condition - MIL). The aircraft stayed in MIL condition for at least 5 seconds.

In Tab. 2 the planned tasks are detailed.

Table 2. Flight conditions and results for flight tests

Task#	Mach	Zp [m]	$max\{\frac{\lvert T_d - T_c \rvert}{T_c}\}$ [1][%]	$max\{\frac{\lvert T_c - T_{mod} \rvert}{T_c}\}$ [2] [%]
1	0,80	5486,4	36,1	7,7
2	0,69	5486,4	24,6	8,7

(1) Maximum absolute error for engines chart relative to calculation
(2) Maximum absolute error for model proposed relative to calculation

3.2.2 Results and analysis

In Fig.7 the variation of thrust is shown for the first task, comparing the thrust curve from kinematic calculation, the proposed model and the thrust obtained from expansion of the engines chart (quasi-static approximation). In Fig.8 a zoom of the region close to the MIL power thrust is shown in detail. It can be observed that the proposed model matches quite well the curve calculated from kinematics, while the engines chart presents always higher values of thrust. In Fig. 9 the error from the proposed model and the engines charts calculation relative the kinematic calculation is shown.

Similar results are obtained in task 2 according to figures 10 to 12.

Overall, the error for not considering the thrust dynamic effects was 28,4% for task 1 and 15.9% for task 2.

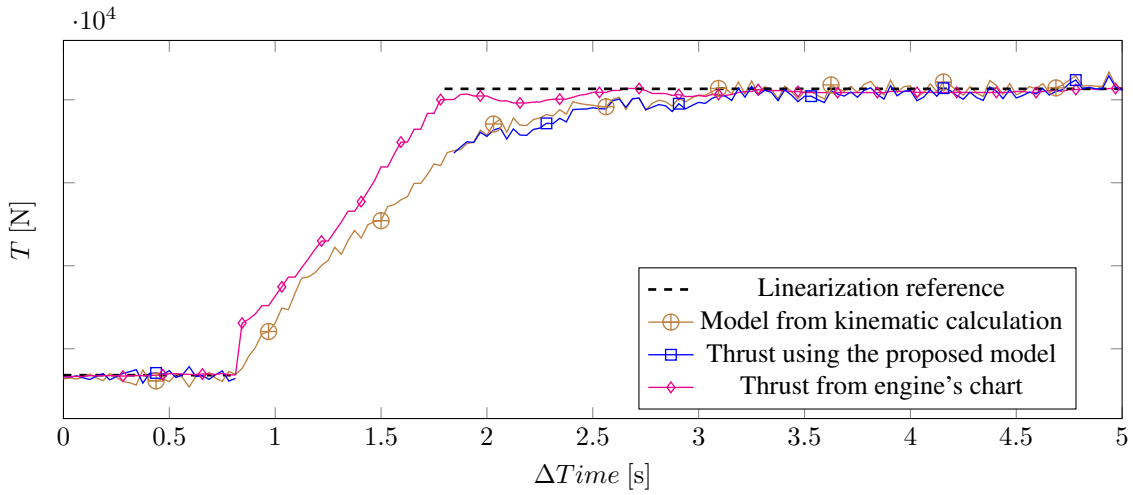

Figure 7. Thrust from cynematic equation, from proposed model and from deck on task 1 flight conditions

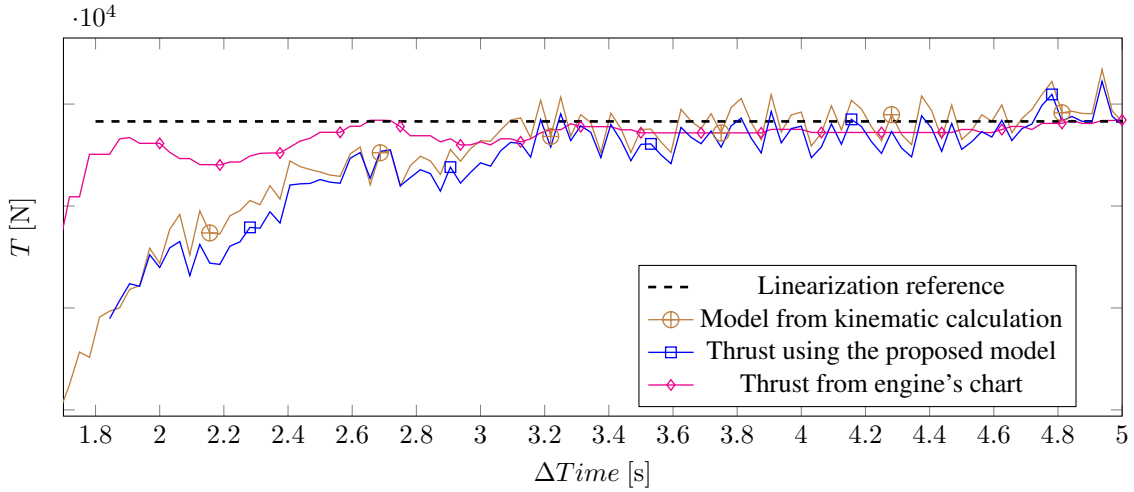

Figure 8. Detail from Fig.7 for MIL condition

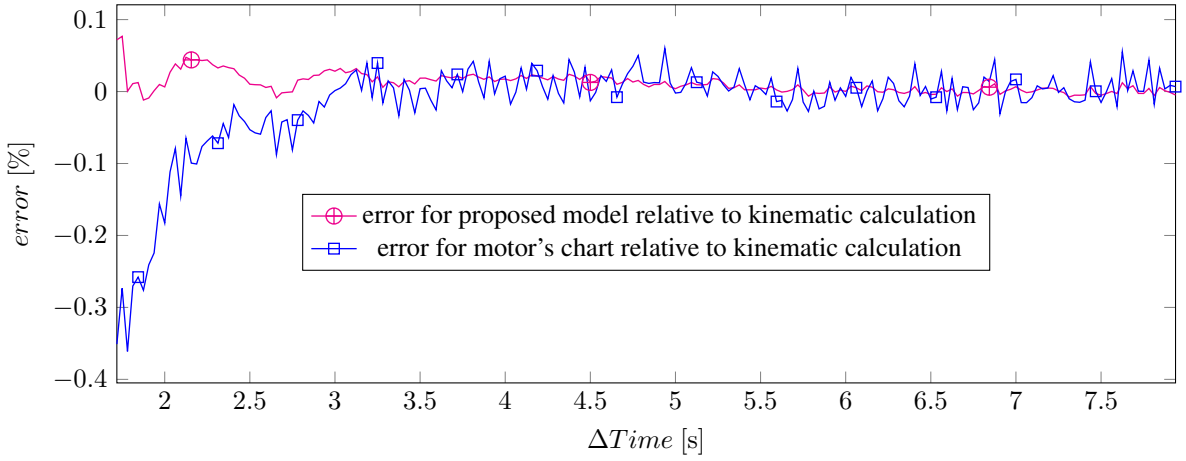

Figure 9. Kinematic equation error in MIL condition for task 1

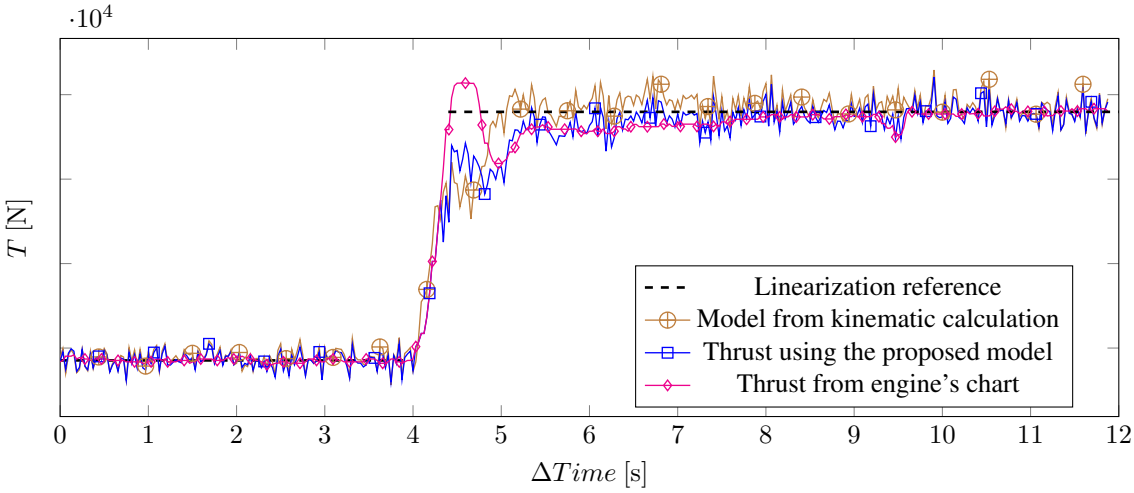

Figure 10. Thrust from kinematic equation, from proposed model and from deck on task 2 flight conditions

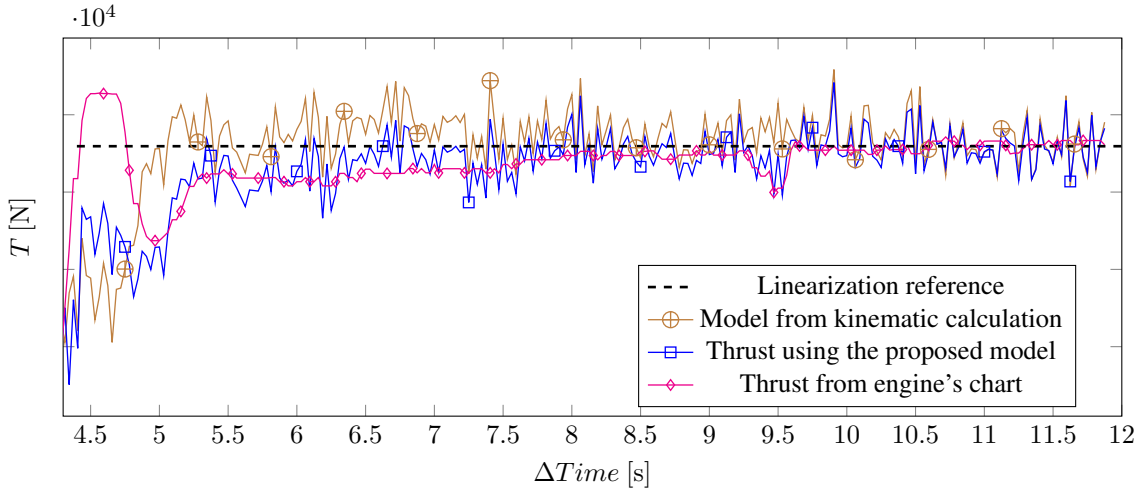

Figure 11. Detail from Fig.10 for MIL condition

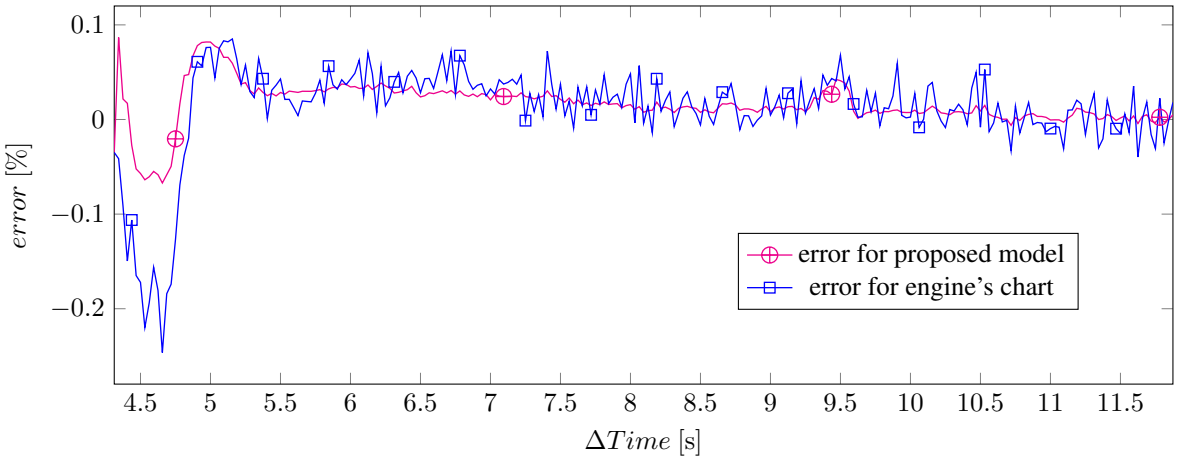

Figure 12. Kinematic equation error in military condition

3.3 CONCLUSIONS

In this work a model to dynamically calculate thrust has been proposed. The presented results showed that the model can be used to represent dynamic effects were the linearity assumption is still valued.

Overall, the error in estimating thrust was reduced in at least 20% in all cases. This shows the potential relevance to apply the proposed model for aircraft with high power-to-weight ratio.

Future works will consider this model to address the impact of thrust dynamics in aircraft dynamic modes.

4. ACKNOWLEDGEMENTS

We acknowledge the support of the Instituto de Pesquisas e Ensaios em Voo (IPEV) for the assistance on the flight test campaigns (operational e technical activities).

5. REFERENCES

Silva, B.G.O., Pinto, M.B.S. and Machado, F.A., 2015. In *Estimation of drag polar in wide mach range from a single continuous dynamic maneuver*. Lancaster, California, USA.

Vinh, N.X., 1999. *Flight mechanics of high-performance aircraft*. Cambridge Aerospace Series, Cambridge, 1st edition.

6. RESPONSIBILITY NOTICE

The authors are the only responsible for the printed material included in this paper.